Sourabh Prakash Roy[1]
***Shubham**[1]**,**
A. K. Singh[1]**,**
R. K. Mehta[1]**,**
O. P. Roy[1]

J. Electrical Systems 19-1 (2023): 82-97

A Systematic Load Frequency Regulation in Two Area Renewable Micro-grid Cluster Utilizing Bald Eagle Search Algorithm

Journal of Electrical Systems

This paper works on the systematic load frequency and tie-lie power transfer regulation within the prescribed limit. The proposed two area renewable energy based micro-grid cluster comprises of dish stirling solar generator, micro hydro turbine, biogas generator as energy generators in area 1. Also, wind turbine, tidal generator, biogas generator as energy generators in area 2. The Flywheel and battery act as mechanical and electrical energy storage devices in their respective areas. Moreover, to make the frequency oscillation die out quickly super magnetic storage devices are connected in the system. A comparison of performance of system with respect to objective function error is made to determine superior controller with minimum error and most stability. The controller parameters is adjusted with Bald eagle search optimizer, Black widow optimizer algorithm, Giza pyramid construction, Teaching learning based optimizer and Genetic algorithm. Lastly, best controller-algorithm i.e. (tilt integral tilt derivative with filter - Bald eagle search optimizer) combination with minimized objective function integral square error is examined under different scenarios.

Keywords: Bald eagle search optimizer, Biogas generator, Dish stirling solar generator, Micro hydro turbine, Tidal generator, Wind turbine.

Abbreviations
MμS – Multi Micro-grid System
DS-SG – Dish Stirling Solar Generator
MHT – Micro Hydro Turbine
WT – Wind Turbine
TG – Tidal Generator
BgT – Biogas Turbine
SMESD – Super Magnetic Energy Storage Device
FESD – Flywheel Energy Storage Device
BESD – Battery Energy Storage Device
SDL – System Dynamic Load
SL – Sensitive Load
TI-TDF – Tilt Integral Tilt Derivative Filter
TIDF-II – Tilt Integral Derivative Filter- Double Integral
PID – Proportional Integral Derivative
PIDN – Proportional Integral Derivative Filter
BESO – Bald Eagle Search Optimization Algorithm
BWOA – Black Widow Optimization
GA – Genetic Algorithm
GPC – Giza Pyramid Construction
TLBO – Teaching Learning Based Optimization

1. Introduction

Renewable energy sources are the alternative to the fossil fuel based conventional sources. They help to meet the ever growing world energy demand. More than one renewable energy sources are connected to form micro-grid cluster as the energy generated

* Corresponding author: Shubham. Department of Electrical Engineering, NERIST, 791109 Itanagar, Arunachal Pradesh, India, E-mail: shubham.roy3@gmail.com
[1] Department of Electrical Engineering, NERIST, 791109 Itanagar, Arunachal Pradesh, India

by single source is not sufficient to meet the load requirement. The multi source multi area makes the cluster more reliable and resilient. Moreover, energy storage devices are connected to the energy sources to improve system performance and stability [1]. The major advantages of renewable sources like safety, efficiency, less global warming, inexhaustibility, improved public health and economic benefits as stable energy prices outweigh its disadvantages like weather uncertainty and unpredictability of renewable sources. This has increased the generation of energy from non-conventional renewable sources [2]. There are a large number of papers, elaborating creation of micro-grid with fossil fuel and renewable energy sources. In [3] describes conventional system consisting modeling of non-reheat thermal in real time simulation software OPAL-RT. This system performs well with 2 Degree Of Freedom TIDF tuned with whale optimization algorithm (WOA) with and without governor dead band. Also, [4-6] describes about multi area power system model with conventional energy sources like thermal-hydro-gas units. The impact of integration HVDC is demonstrated in [7]. The detailed modeling of PV and wind sources with energy storage and load forming a stable system in discussed in [8, 9]. The extended modeling of integration of conventional and renewable sources in two area is given in [10]. Thermal-hydro-gas are the component of conventional sources where as wind and solar energy made the renewable energy portion. An effort is also made to make the micro-grid more realistic with the inclusion of rate constraints, dead band, delays and uncertainties present in the system.

Penetration of multi renewable energy sources in the system results in large frequency and tie-line power overshoot. This deviation because of the energy imbalance is mitigated using frequency regulation controller. The fundamental frequency regulators are having the gain of proportional, integral and derivative. All other controllers are built with the combinations of the aforementioned controllers. In [11, 26, 27] authors has demonstrated stabilization of cluster of hydrothermal plant with wind/diesel generator/aqua electrolyser/fuel cell/battery as its components. Controller employed are PID with 2 or 3 degree of freedom, PIDF, FOPID, PI-PID, TID and CC-TID. FOPID is the controller which is explained by the concept of Oustaloup, Carlson, Matsuda, and continued fraction expansion for s-domain approximation as discussed in [12]. In [13] purely renewable energy based stand alone micro-grid is evaluated with some of the derived complex controller namely PIDF-(1+I) PID, PIDF, and PIDF-(1+I). Furthermore, application of cascade multistage controller in hybrid micro-grid system with multi area units is presented in [14]. Wind farm integrated with electric vehicle and system frequency is stabilized with 2 degree of freedom PID tuned with robust internal mode control (IMC) is provided in [9]. Some other optimization techniques for example sliding mode control [16], Model predictive control [8, 15], terminal sliding mode control [17], adaptive sliding mode control [18] and artificial neural network methods [19] help in improving the controller tuning and subsequently its performance.

After, an appropriate controller is sorted out; its gain parameters are tuned using advanced optimization techniques. A quest for newer and better optimization techniques is becoming an emerging field for the researches. Number of optimization algorithm is utilized for the frequency and tie-line power transfer management in MμS. Some of the present day intelligent algorithms developed are Modified sine cosine algorithm (MSCA) [20], Grasshopper algorithmic technique (GOA) [21] and Modified salp swarm algorithm

(MSSA) [22] introduced by Shubham Gupta et.al., Laith Abualigah et.al. and Walaa H. El-Ashmawi et.al. respectively. Movable damped wave algorithm (MDVA) [23] developed in 2019 and Chaotic crow search algorithm (CCSA) [21] developed in 2018 by Rizk M. Rizk-Allah et.al. Also, Afshin Faramarzi et.al. developed Marine predators' algorithm (MPA) [25] and Equilibrium optimizer (EO) [6] in 2020 and 2019 respectively. The present work includes optimization algorithm namely Bald eagle search optimization (BESO) [24, 28], Black widow optimizer algorithm (BWOA) [30], Giza pyramid construction (GPC) [29], Teaching learning based optimization (TLBO) [32] and Genetic algorithm (GA) [31]. These algorithms are employed to adjust PID, PIDN, TIDF II and TI-TDF. The main benefits of algorithm optimization are accurate, rapid convergence rate and preventing local optimum solutions for the micro-grid clusters. Also, BESO is not being used to control load frequency in DS-SG/Micro-Hydro/Wind/Tidal/ Biogas Based Renewable Micro-grid Cluster with tilt order control. The major focus of this paper is made to select best optimization algorithm for the proposed controller with minimum objective function in the two area renewable energy micro-grid cluster. The works done to fulfill the objective of paper are as follows –

(i) Development of dish stirling solar generator, micro hydro generator, wind generator, tidal generator and biogas generator based two area renewable energy micro-grid cluster.
(ii) Designing and selection of appropriate controller among the proposed controller namely PID, PIDN, TIDF II and TI-TDF based on minimum objective functions.
(iii) Tuning controller parameters with algorithms namely BESO, BWOA, GPC, TLBO and GA in order to compare various control strategies and algorithms.
(iv) Evaluation of superior controller algorithm combination with minimum objective functions under different scenarios.
(v) Determination of steady state and transient parameters for the frequency and tie-line power profile.

The remaining portion of the paper is organized as follows. The whole configuration description of the proposed system is provided in section 2. Moving further, controller design scheme and selection of objective function is elaborated in section 3. Also, section 4 gives details of the steps of the algorithms utilized to tune the controller parameter. After, this time based evaluation and result analysis is covered in section 5 and 6 respectively. Lastly, section 7 explains the conclusion and there after references.

2. Description of proposed micro-grid cluster

2.1 Dish Stirling solar generating unit (DS-SG)

DS-SG is an electrical energy producing unit which comprises up of a concave parabolic dish, cavity receiver and stirling heat engine with generating unit. The solar dish rotates in such a direction so as to throw back the optimal amount of sun ray to the receiver. This results in increasing the temperature of receiver as well as engine. The piston attached to engine converts the energy of working gas such as hydrogen or helium into electrical energy. The description of DS-SG transfer function is given in equation (1), where, $K_{DS\text{-}SG}$, $T_{DS\text{-}SG}$ is DS-SG valve gain and valve time constant whose values are 1 and 5 respectively.

$$G_{DS\text{-}SG}=\left(\frac{K_{DS\text{-}SG}}{1+sT_{DS\text{-}SG}}\right) \quad (1)$$

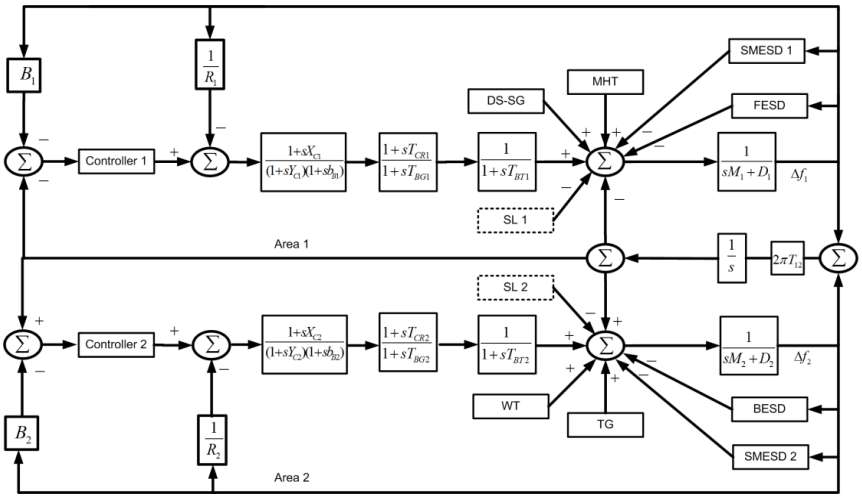

Fig 1. Schematic diagram of proposed two area system

2.2 Micro hydro turbine generating unit (MHT)

Micro hydro unit generates the electrical energy from the kinetic flow of the water. The standard power generated from MHT is of 5-100 KW capacity [35]. The linearized MHT transfer function description is given in equation (2), where, K_{MHT}, T_{MHT}, K_{PH}, T_{PH}, T_W are MHT governor gain and time constant, penstock gain and time constant, turbine time constant whose values are 0.5, 0.2, 5, 28.75 and 1 respectively.

$$G_{MHT}=\left(\frac{K_{MHT}}{1+sT_{MHT}}\right)\left(\frac{K_{PH}}{1+sT_{PH}}\right)\left(\frac{-1+sT_W}{1+0.5sT_W}\right) \quad (2)$$

2.3 Energy storage devices area 1- flywheel energy storage devices (FESD)

In case of malfunctioning of generating sources, energy storage devices are connected in the system as a secondary energy producing unit. In the present work, flywheel is interconnected in area 1 of microgrid. The linearized mathematical description of function FESD is expressed as in equation (3), where, T_C, T_{CM}, T_{DM} are flywheel converter time constant , command measurement time constant and delay measurement time constant whose values are 0.1, 0.001 and 0.1 respectively.

$$G_{FESD}=\left(\frac{1}{1+sT_C}\right)\left(\frac{1}{1+sT_{CM}}\right)\left(\frac{1}{1+sT_{DM}}\right) \quad (3)$$

2.4 Wind turbine generating unit (WT)

The generating power from wind plants is considered one of the fully grown and promptly developing renewable energy sources [14]. The mechanical power derived from WT i.e. P_{MWT} can be articulated as equation (4),

$$P_{MWT}=0.5C_P(\lambda,\beta)\rho A_B v^3 \quad (4)$$

where, C_P is turbine power conversion coefficient of WT which is the function of tip to speed ratio λ and pitch angle β, ρ is air density in kg per cubic meter, A_B is blade swept area in meter square and v is wind speed in meter per second. The key factor in deciding the

amount of mechanical power is wind speed which is summation of base wind speed, gust wind speed, ramp wind speed and noisy wind speed. The transfer function for the WT is expressed as equation (5), where, K_{WT}, T_{WT} are WT gain and time constant whose values are 1, 1.5 respectively.

$$G_{WT}=\left(\frac{K_{WT}}{1+sT_{WT}}\right) \tag{5}$$

2.5 Tidal generating unit (TG)

An on-seashore TG is an upcoming renewable energy source. Its working principle and control techniques are identical to WT [37]. The mechanical output from TG i.e. P_{MTG} can be presented as equation (6),

$$P_{MTG}=0.5\rho_W \pi r^3 \nu_T C_{TG}(j,\beta) \tag{6}$$

where, ρ_W is water density in kg per cubic meter, r is the turbine blade radius, ν_T is tidal speed in meter per second, C_{TG} is turbine power conversion coefficient, Φ is tip to speed ratio and β is the pitch angle. The transfer function of TG is as follows, equation (7), where, K_{TG}, T_{TG} are TG gain and time constant whose values are 1, 0.08 respectively.

$$G_{TG}=\left(\frac{K_{TG}}{1+sT_{TG}}\right) \tag{7}$$

2.6 Energy storage devices area 2 - battery energy storage devices (BESD)

BESD is a type of ESD which stores electrical energy in the form of chemical energy. It confers the reserved energy to minimize the mismatch in power generation and load demand [36]. Thus, act as assistance to the prime generating sources at the time of necessity. The linearized transfer function of BESD is indicated in equation (8), where, T_C, T_{CM}, T_{DM} are flywheel converter time constant, command measurement time constant and delay measurement time constant whose values are 0.1, 0.001 and 0.1 respectively.

$$G_{BESD}=\left(\frac{1}{1+sT_C}\right)\left(\frac{1}{1+sT_{CM}}\right)\left(\frac{1}{1+sT_{DM}}\right) \tag{8}$$

2.7 Biogas turbine generating unit (BgT)

BgT is the renewable bio-degradable energy source which utilizes human and animal wastes. The anaerobic fermentation of bio-degradable wastes results in the production of biogas. These produced biogas mainly consist of carbon dioxide, methane, hydrogen sulphide, siloxanes and moistures. The oxidation of biogas ingredients releases heat and energy which can be utilized as fuel in BgT [38, 39]. The major components of BgT are fuel system and combustor, valve actuator, speed governor and turbine. The output power from BgT is proportional to the input fuel valve so, the transfer function of the BgT can be approximated as equation (9), where, X_C, Y_C, b_B, T_{CR}, T_{BG} and T_{BT} are Lead time. Lag time, valve actuator, combustion reaction time constant, biogas time constant and turbine time constant whose values are 0.6, 1, 0.05, 0.01, 0.23, and 0.2 respectively.

$$G_{BgT}=\left(\frac{1+sX_C}{(1+sY_C)(1+sb_B)}\right)\left(\frac{1+sT_{CR}}{1+sT_{BG}}\right)\left(\frac{1}{1+sT_{BT}}\right) \tag{9}$$

2.8 Super Magnetic Energy Storage Device (SMESD)

SMESD is a super fastly acting energy storage device connected in the system. It is made up of superconducting inductor storing energy in the form of magnetic energy [40]. Compared to other ESD, it supports to damp out the system deviation quickly.The mathematical description of SMESD is given by equation (10), where, T_{S1}, T_{S2}, T_{S3}, T_{S4}, K_{SMESD}, T_{SMESD} are time constant of device compensator, SMESD's gain and time constant whose values are 0.121, 0.8, 0.011, 0.148, 0.297, 0.03 respectively.

$$G_{SMESD}=\left(\frac{1+sT_{S1}}{1+sT_{S2}}\right)\left(\frac{1+sT_{S3}}{1+sT_{S4}}\right)\left(\frac{K_{SMESD}}{1+sT_{SMESD}}\right) \tag{10}$$

2.9 System dynamic load (SDL)

The mismatch in overall power generated and gross load requirement leads to fluctuation in frequency and tie-line power transfer [41]. The power balance equations of two area proposed system is given by equation (11) and (12) respectively.

$$\Delta P_{G1}=\Delta P_{S}+\Delta P_{MT}+\Delta P_{BG}\pm\Delta P_{FS}\pm\Delta P_{SM1}-\Delta P_{L1}-\Delta P_{12} \tag{11}$$

$$\Delta P_{G2}=\Delta P_{W}+\Delta P_{T}+\Delta P_{BG}\pm\Delta P_{BS}\pm\Delta P_{SM2}-\Delta P_{L2}-\Delta P_{21} \tag{12}$$

where, ΔP_{G1}, $\Delta P_{s,}$ $\Delta P_{MT,}$ $\Delta P_{BG,}$ ΔP_{FS}, $\Delta P_{SM1,}$ $\Delta P_{L1,}$ $\Delta P_{12,}$ ΔP_{G2}, $\Delta P_{W,}$ $\Delta P_{T,}$ $\Delta P_{SM2,}$ $\Delta P_{L2,}$ ΔP_{21} are power generated in area 1, power generated from DS-SG, power generated from MHT, power generated from BgT, power stored in FESD, power stored in SMESD in area 1, load demand in area 1, tie-line power transferin area 1 and 2, power generated in area 2, power generated from WT, power generated from TG, power stored in BESD, power stored in SMESD in area 2, load demand in area 2, tie-line power transferin area 2 and 1 respectively. The comprehensive transfer function of the rotating mass dynamics i.e. G_{RMD} can be expressed as equation (13), where, D, M are Damping factor and inertia constant whose values are 0.012, 0.2 respectively.

$$G_{RMD}=\left(\frac{1}{D+sM}\right) \tag{13}$$

2.10 Sensitive load (SL)

In both the area, SL is a step changing load whose magnitude is taken as 0.04 pu for 0 to 100 seconds and increases from 0.04 to 0.05 pu at 100 seconds. It remains at 0.05 pu for the rest of the simulation period of 200 seconds.

3. Controller design scheme

The controller employed in order to optimize DS-SG/MHT/WT/TG/Biogas based two area renewable energy micro-grid cluster are PID, PIDN, TIDF II [28] and TI-TDF [35]. The proposed main controller TI-TDF is a 7 variable controller whose transfer is given by equation (14),

$$\frac{\Delta P}{\Delta f}=K_{T1}s^{-\frac{1}{\lambda_1}}+K_{I}s^{-1}+K_{T2}s^{-\frac{1}{\lambda_2}}+sK_{D}\frac{N_c}{s+N_c} \tag{14}$$

The mathematical description of other aforementioned controllers is tabulated in table 1. The section is dedicated to select an appropriate, well organized and efficient controller strategy. This will result in stabilization of the frequency and tie-line transfer power limit within the prescribed range. The controller parameters are tuned with BESO, BWOA, GPC,

TLBO and GA within the constraints of objective function, upper and lower bounds. The values of the parameter with the corresponding lower-upper boundary conditions for PID, PIDN, TIDF II and TI-TDF thus obtained is provided in table 2, table 3, table 4 and table 5 respectively.

The performance of these controllers after tuning is evaluated with the objective function formulation. The appropriate selection of objective function is very much necessary for minimizing the transient and steady state response of the system. The objective function family consists up of integral square error (ISE), integral time square error (ITSE), internal absolute error (IAE) and integral time absolute error (ITAE). Table 6 depicts the comparison of controller with regard to predefined objective functions. It has been noted from table 6, that all the controller shows minimum error for ISE. Also, among the controller TI-TDF gives minimal error for ISE objective functions. Thus, the system stabilization with BESO based TI-TDF controller gives improved results than other controller-algorithm combinations.

Table 1. Proposed controllers mathematical description

PID	PIDN	TIDF-II
$\frac{\Delta P}{\Delta f}=K_P+K_I s^{-1}+sK_D$	$\frac{\Delta P}{\Delta f}=K_P+K_I s^{-1}+sK_D\frac{N_c}{s+N_c}$	$\frac{\Delta P}{\Delta f}=K_{T1}s^{-\frac{1}{\lambda_1}}+K_{I1}s^{-1}+sK_D\frac{N_c}{s+N_c}+K_{I2}s^{-2}$

Table 2. PID controller tuned gain and J_{ISE}

Algorithm	PID controller gain values						
	J_{ISE}	K_{P1}	K_{P2}	K_{I1}	K_{I2}	K_{D1}	K_{D2}
(LB)	-	0	0	0	0	0	0
(UB)	-	300	300	300	300	300	300
BESO	0.0016238	272.545	207.637	180.381	10.1187	133.148	130.970
BWOA	0.0016834	169.070	272.569	24.5177	184.264	162.647	108.624
GPC	0.0017053	185.071	300	159.452	207.603	10.7686	159.035
TLBO	0.0016088	249.745	253.450	18.0194	241.249	131.022	137.491
GA	0.0017034	242.282	179.526	20.2100	109.506	147.181	206.568

Table 3. PIDN controller tuned gain and J_{ISE}

Algorithm	PIDN controller gain values								
	J_{ISE}	K_{P1}	K_{P2}	K_{I1}	K_{I2}	K_{D1}	K_{D2}	N_1	N_2
(LB)	-	-	0	0	0	0	0	0	0
(UB)	-	-	300	300	300	300	300	300	300
BESO	0.0021667	0.0022	299.99	275.790	2.96	29.467	2.74	0.114	22.650
BWOA	0.0317650	0.0318	300	0	0	0	0	0	0
GPC	0.0024091	0.0024	300	300	0.001	0.0003	0	0	0
TLBO	0.0019812	0.0020	261.40	261.396	14.436	14.436	0.553	0.553	186.640
GA	0.0023470	215.78	0.9276	60.7430	256.04	124.041	0.501	104.784	248.300

Table 4. TIDF II controller tuned gain and J_{ISE}

Algorithm	TIDF II controller gain values						
	J_{ISE}	K_{T1}, K_{T2}	λ_1, λ_2	K_{I11}, K_{I21}	K_{D1}, K_{D2}	N_1, N_2	K_{I12}, K_{I21}
LB	-	0	0	0	0	0	0
UB	-	300	1	300	300	300	1

BESO	0.001556	297.7982	0.3135	2.2337	161.8136	235.336	0.11390
		220.3397	0.3832	13.0943	167.1383	275.439	0
BWOA	0.322270	15.0951	0.3942	15.8305	0	88.9693	11.10810
		18.7843	0	206.374	233.2991	95.3012	299.4173
GPC	0.001875	300	0	249.891	129.3389	300	0.000061
		0	0.1679	0	0.172702	0.00024	0
TLBO	0.0015350	290.0755	0.2599	0.001900	174.1497	290.591	0.115900
		300.0000	0.2641	226.9588	183.0184	280.470	0.436800
GA	0.002969	208.4486	0.3171	285.0666	10.3338	131.623	114.4675
		229.6550	0.7952	56.0618	146.9293	133.676	193.8939

Table 5. TI-TDF controller tuned gain and J_{ISE}

Algorithm	TI-TDF controller gain values							
	J_{ISE}	K_{T11}, K_{T21}	$\lambda_{11}, \lambda_{12}$	K_{I1}, K_{I2}	K_{T12}, K_{T22}	$\lambda_{12}, \lambda_{22}$	K_{D1}, K_{D2}	N_1, N_2
LB	-	0	0	0	0	0	0	0
UB	-	300	1	300	300	1	300	300
BESO	0.0015205	104.8794	0.3086	9.0935	221.3285	0.1926	148.9353	299.4340
		262.5026	0.4042	38.561	184.2763	0.3930	169.8233	298.4546
BWOA	0.0017086	188.7154	0.0429	190.96	186.6868	0.1963	118.1858	183.2870
		185.0515	0.1249	23.037	159.2992	0.1513	58.13550	82.6168
GPC	0.001670	300	0.0083	300	0	0	170.346	300
		58.4095	0.5307	0.2167	280.203	0	170.647	300
TLBO	0.0015537	300.0000	0.1896	10.792	27.3041	0.2912	151.6426	189.7433
		101.4303	0.3736	122.32	218.9323	0.0954	143.0246	294.2324
GA	0.0017399	252.2152	0.2543	244.29	73.0575	0.9293	104.9951	58.9786
		75.3252	0.6160	141.99	105.4979	0.8308	175.5792	164.9171

Table 6. Analysis of objective functions for proposed controller tuned with BESO

Controller	Dimensions	J_{ISE}	J_{ITSE}	J_{IAE}	J_{ITAE}
PID	6	0.001624	0.01492	0.1938	11.01
PIDN	8	0.002167	0.04920	0.3679	39.80
TIDF II	12	0.001557	0.01419	0.1831	10.71
TI-TDF	14	0.001520	0.01345	0.1786	10.87

4. Bald eagle search optimization algorithm

Bald Eagle Search optimisation Algorithm abbreviated as BESO is an advanced algorithm developed by H. A. Alsattar et al in 2019. This meta heuristic algorithm is a based on the natural hunting methodology of raptor Bald eagle. The entire hunting techniques of the eagle can be classified into three parts which includes locating appropriate space full of food in the nearby area, searching for best swooping for particular prey by spirally above in the sky and lastly, accelerating towards the prey from best location. The detailed steps and equations involved for the BESO algorithm are as follows -

(i) Initialization of the controller dimensions, boundary constraints, maximum iterations and search agent.

(ii) Arbitrarily chose an initial point and calculation of fitness function.

(iii) Chose the best area by assessing the equation

$$Z_{new(i)} = Z_{best} + \alpha * rand(Z_{mean} - Z_i)$$

(iv) Update the best swooping area by assessing the equation

$$Z_{new(i)}=Z_i+y(i)*(Z_i-Z_{i+1})+x(i)*(Z_i-Z_{mean})$$

(v) The acceleration of eagle from swooping location towards the prey is updated by equation

$$Z_{new(i)}=rand*Z_{best}+x_1(i)*(Z_i-c_1*Z_{mean})+y_1(i)*(Z_i-c_2*Z_{best})$$

where, the constants are defined as a ∈ [5, 10] dictates the corner between search points, R ∈ [0.5, 2], establishes the search cycles, $c_1,c_2 \in [1, 2]$, $\theta(i)=a*\pi*rand$, $r(i)=\theta(i)+R*rand$, $\theta(i)=a*\pi*rand$ and $r(i)=\theta(i)$. Also, some factors are calculated by $x(i)=\frac{r(i)*\sin(\theta(i))}{\max(|r(i)*\sin(\theta(i))|)}$, $y(i)=\frac{r(i)*\cos(\theta(i))}{\max(|r(i)*\cos(\theta(i))|)}$ and $x_1(i)=\frac{r(i)*\sinh(q(i))}{\max(|r(i)*\sinh(q(i))|)}$.

It is necessary to have a proper selection of controller tuning algorithms to provide efficient, fast parameter calculating and less time consuming optimization procedure. The proposed renewable energy system is stabilized in two area micro-grid cluster with BESO [28], BWOA [30], GPC [29], TLBO [32] and GA [31]. The convergence curve of the mentioned algorithm obtained with 5 search agent and maximum iteration of 100 is provided by figure 2.

Table 7. Algorithms parameters

Algorithms	Parameters
BESO	$c1, c2 \in [1,2]$, $\alpha = 2$, $a = 10$, $R = 1.5$
BWOA	$ß_2 \in (-1,1)$, $m \in (0.4,0.9)$
GPC	Constants
TLBO	$r_i \in [0,1]$
GA	$P_m = 0.01$, $P_c = 0.8$, tournament selection
Common Parameters	Maximum iterations = 50, Search agent size = 5, simulation time = 200 seconds

The essential parameters, maximum iteration, population size and simulation time period utilized for optimization are outlined in Table 7. It has been observed from Fig 2. that the execution of BESO is step ahead from other optimization algorithms. Moreover, different case studies that have been implemented with the help of BESO optimization approach also justifies the superiority of BESO.

Table 8. Comparison of transient parameters of frequency and tie-line power transfer

Transient Parameters		PID	PIDN	TIDF II	TI-TDF
Overshoot	Δf_1	1.525×10^{-2}	1.823×10^{-2}	1.009×10^{-2}	1.248×10^{-2}
	Δf_2	8.015×10^{-3}	5.89×10^{-2}	5.702×10^{-3}	1.142×10^{-2}
	ΔP_{12}	2.218×10^{-3}	3.335×10^{-3}	3.738×10^{-4}	5.687×10^{-4}
Undershoot	Δf_1	-4.466×10^{-2}	-5.88×10^{-3}	-4.447×10^{-2}	-4.467×10^{-2}
	Δf_2	-3.843×10^{-2}	-4.67×10^{-3}	-3.803×10^{-2}	-3.785×10^{-2}
	ΔP_{12}	-1.195×10^{-3}	-3.54×10^{-3}	-1.332×10^{-3}	-2.137×10^{-3}

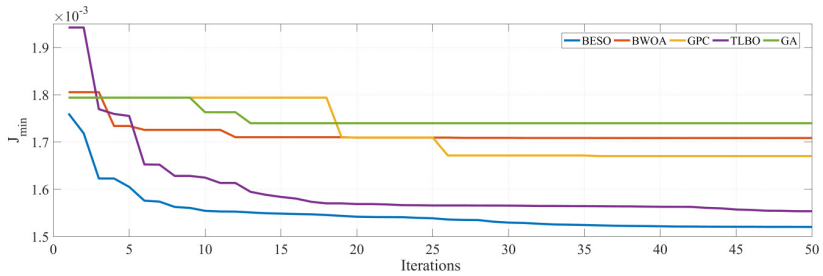

Fig 2. Comparison of convergence curve of BESO, BWOA, GPC, TLBO and GA algorithm.

5. Case studies

Case 1: Normal condition

An effort is made to analyse the various cases that may arise in different situations in the system and explained in this section. In normal cases, all the generating sources like DS-SG, MHT, BgT of area1 and WT, TG, BgT of area 2 are perfectly working and supplying adequate power to the system dynamic as well as sensitive load. Fig 3 and 4 plots power from DS-SG as P_S, MHT as P_{MT}, BgT as P_{BG}, WT as P_W, TG as P_T, FESD as P_{FS}, BESD as P_{BS}, SMESD as P_{SM}, DL as P_L , frequency variations i.e. f_1 and f_2 and tie-line power P_{12} response for area 1 and area 2 respectively. Initially, for area1, when generating units are about to generate power and taking as SDL = 0.04 pu till 100 seconds. All the required power is given by FESD and SMESD till the BgT starts to supply the load. It results in initial downward transients in the frequency and tie-line power response which varies around zero after sometime as shown in Fig 3.

Later on, when P_S is fluctuating around 0.05 pu thus supply the SDL and P_{BG}, P_{FS}, P_{SM} reduces to zero till 100 seconds. The frequency and tie-line power transferresponse just vary around zero. At 100 seconds, when there is sudden rise in SDL from 0.04 pu to 0.05 pu, there is a mismatch in generation and demand. To minimize this mismatch storage devices and BgT supplies the remaining required power requirement. Furthermore, after 120 seconds when SDL is the same but P_S is decreasing, the P_{BG} gradually increases to meet the load demand till the end of 200 seconds as shown in Fig 6.

Similarly, for area 2, P_W and P_T are gradually increased during 0 to 50 seconds. SDL is 0.04 pu during this phase, so BESD, SMESD and BgT are providing power to the SDL. Later on, during the peak generation period, P_{BS}, P_{SM}, P_{BG} reduces to zero and all the power requirement is provided by combination of P_W and P_T. After 100 seconds, there is increase in SDL, decrease in P_W, P_T, so BgT provides the required power. The f_2 shows an initial dip in the initial phase after that it varies around zero for the rest of the simulation period as shown in Fig 4.

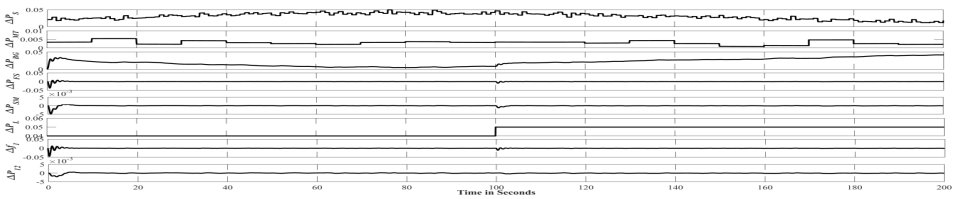

Fig 3. Response of change in input power generation, load, frequency and tie-line power transfer for area 1

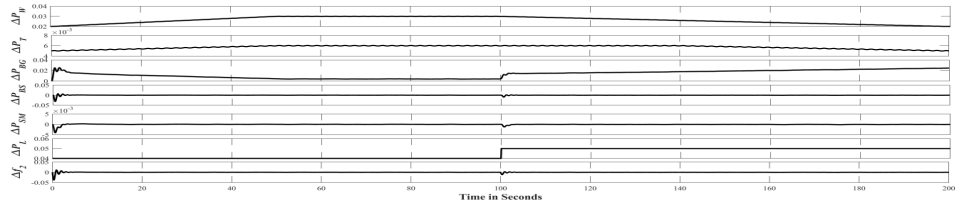

Fig 4. Response of change in input power generation, load, frequency and tie-line power transfer for area 2

Case 2: Absence of MHT in area 1 and TG in area 2

This situation may emerge due to non- functioning of MHT in area 1 and TG in area 2 which occurs due to imbalance in the system response as demonstrated in Fig 5 and 6. The increase in sDL is supplied by DS-SG, ESD and BgT for area 1 and WT, ESD and BgT for area 2. The system response for the situation is given in Fig 5 and 6. It is observed that deviation in frequency and tie-line power transferdue to mismatch in power equilibrium is under admissible limits. Also, the first drop in the frequency of the both the area damps out its oscillation after few cycles.

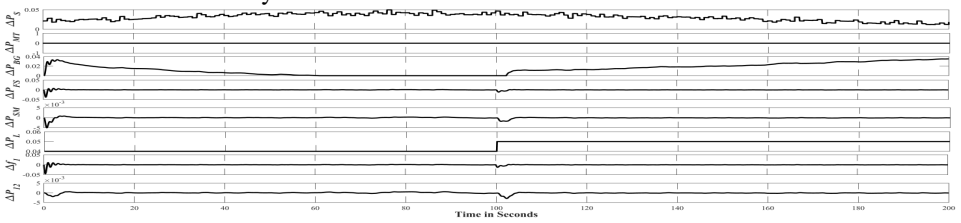

Fig 5. Response of change in input power generation, load, frequency and tie-line power transfer for area 1

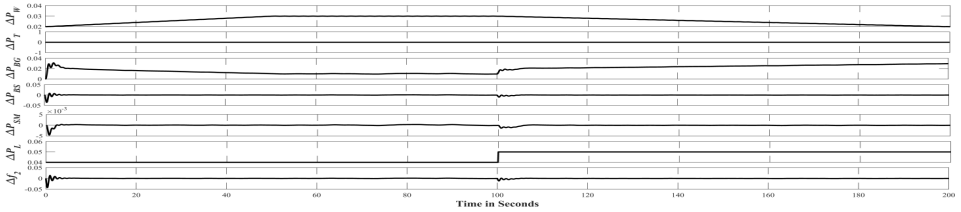

Fig 6. Response of change in input power generation, load, frequency and tie-line power transfer for area 2

Case 3: Absence of DS-SG as well as MHT in area 1 and WT as well as TG in area 2

The improper functioning of DS-SG and WT occurs at night and due to non-availability of wind respectively. Also, abnormality in hydrological cycle can lead to non-functioning of MHT and TG. The system response in such situation is depicted in Fig 7 and 8. The increase in SDL is endowed by ESD initially and later on energy is solely provided by BgT in both the area. The dip in frequency observed during increase in DL which is under permissible limits and settle down after few cycles.

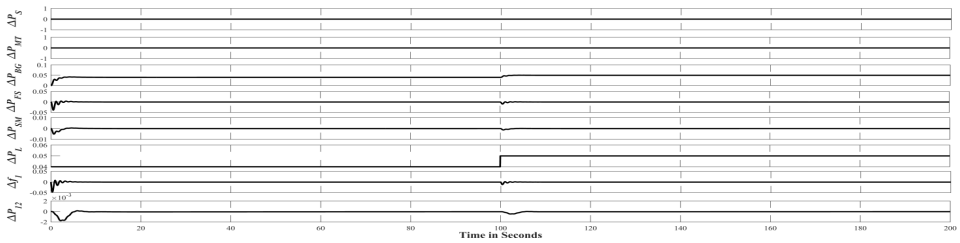

Fig 7. Response of change in input power generation, load, frequency and tie-line power transfer for area 1

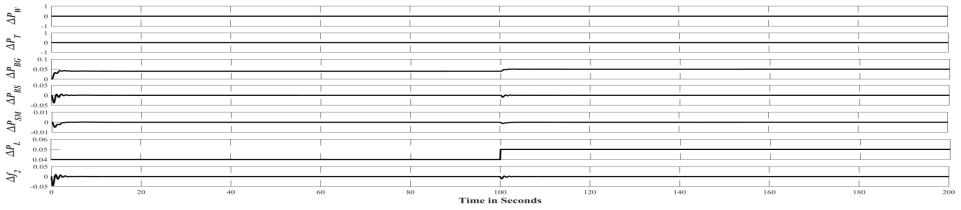

Fig 8. Response of change in input power generation, load, frequency and tie-line power transfer for area 2

Case 4: Presence of all sources with random load changing

This last situation is considered to check the sensitivity of the system towards the random changing load. It will give us information about the robustness of the controller towards the changing disturbance of the system. In this condition, all the generating sources are available in both the areas. The major difference between case 1 and case 4 is that the DL is step changing load in former whereas in later, the SDL is a random changing pattern which is shown in Fig 9 and 10. The power demanded by load is mainly supplied by DS-SG (for area 1) and WT (area 2). The unused excess power generated is stored in the ESD which is used during peak load demand. It has also been observed from frequency and tie-line power transferresponse settles down quickly in both areas due to robust nature of the controller.

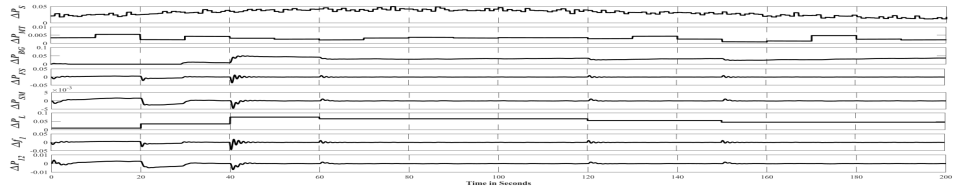

Fig 9. Response of change in input power generation, load, frequency and tie-line power transfer for area 1

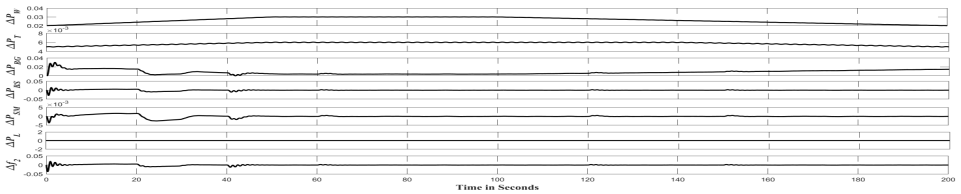

Fig 10. Response of change in input power generation, load, frequency and tie-line power transfer for area 2

6. Result analysis

The DS-SG/MHT/WT/TG/biogas turbine based two area renewable energy micro-grid system is executed in MATLAB 2016 software for a 200 seconds simulation time period. The system is stabilized using PID, PIDN, TIDF-II and TI-TDF. The parameters of these controllers are optimized with BESO, BWOA, GPC, TLBO and GA with the five number of search agent and 100 as maximum iteration. The lower bound constraints for tuning the controller are 0 for all the controller parameters whereas upper bound is 1 for tilt parameter and 300 for the remaining. Following observations were made for the system regarding its performance -

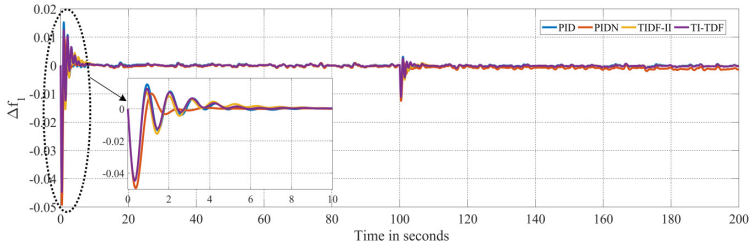

(a) Frequency profile area 1

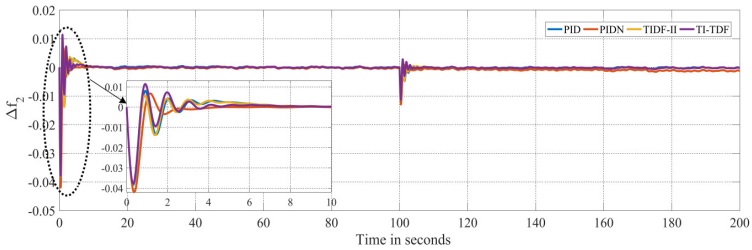

(b) Frequency profile area 2

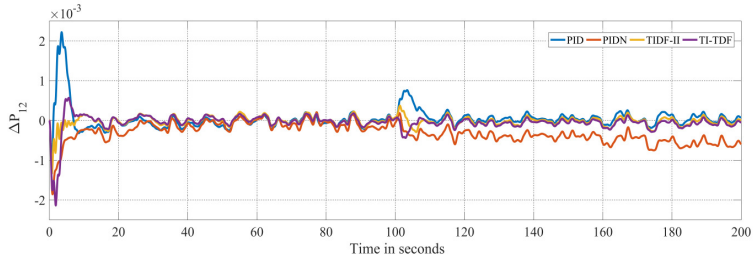

(c) Tie-line power transfer profile

Fig 11. Micro-grid cluster profile of BESO tuned PID, PIDN, TIDF II and TI-TDF controller in proposed system

(i) Table 6 showing comparison of objective function with BESO, it has been noted that the maximum error in objective function is 39.89 for PIDN with ITAE and minimum is 0.001520 for TI-TDF with ISE. Moreover, ISE is showing minimal value of error for all the controller among the family of objective function.

(ii) The superior controller is selected based on the minimum error in steady state and transient parameters as depicted in table 2, 3, 4, 5 and 8. So, it is concluded that TI-TDF when tuned with BESO gives superior performance compared to other proposed controllers.

(iii) The algorithm's convergence curve as well as from frequency and tie-line power profile as per figure 10 helps in deciding the efficient and less time consuming algorithm for the controller. It is observed that proposed algorithm is providing best result in all the proposed controller.

(iv) It has been observed from figure 11(a) & (b) and table 8, that the minimum in frequency profile for the system is given by BESO tuned TI-TDF controller. Also, the maximum and minimum shoot for BESO tuned TI-TDF in frequency profile is 4.467 x10^{-2} and 1.142 x10^{-2} respectively.

(v) The minimal shoot in tie-line power transfer for the system is given by BESO tuned TI-TDF controller as supported by figure 10(c) and table 8. Also, the maximum and minimum shoot for BESO tuned TI-TDF in tie-line power profile is 2.137 x10^{-3} and 5.687 x10^{-4} respectively.

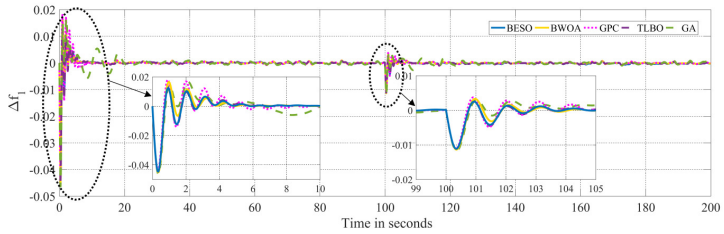

(a) area 1

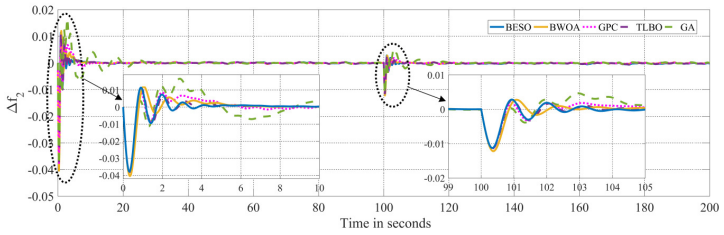

(b) area 2

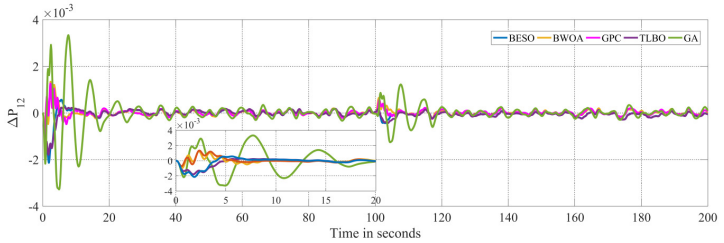

(c) Tie-line transfer of power between area 1 and area 2 profile

Fig 12. Micro-grid frequency profile of BESO, BWOA, GPC, TLBO and GA

7. Conclusion

The paper studies the collaborative load frequency regulation in two area micro-grid systems consisting up of DS-SG, MHT, WT, TG and BgT as the renewable energy generators. Also, FESD, BESD, and SMESD are included in the proposed system as energy storage devices. Initially, efforts have been made to select the superior algorithm from convergence curve. Next step is to determine effective control strategy and its parameter is tuned with BESO, BWOA, GPC, TLBO and GA. From different case studies and study of system frequency as well as tie-line power profile, it is has been concluded that BESO

tuned TI-TDF controller is superior to other controllers. This work can be further on extended to employment of weighted objective function, incorporation of communication time delays, generation rate constraints and generation band constraints with recent controllers and algorithms combinations to the previous works.

References

[1] Da Rosa, Aldo Vieira, and Juan Carlos Ordóñez. *Fundamentals of renewable energy processes*. Academic Press, 2021.

[2] Ramesh, Maloth, Anil Kumar Yadav, and Pawan Kumar Pathak. "An extensive review on load frequency control of solar-wind based hybrid renewable energy systems." *Energy Sources, Part A: Recovery, Utilization, and Environmental Effects* (2021): 1-25.

[3] Güler, Yavuz, and Ibrahim Kaya. "Load Frequency Control of Single-Area Power System with PI–PD Controller Design for Performance Improvement." *Journal of Electrical Engineering & Technology* (2023): 1-16.

[4] Shakibjoo, Ali Dokht, Mohammad Moradzadeh, Seyed Zeinolabedin Moussavi, Ardashir Mohammadzadeh, and Lieven Vandevelde. "Load frequency control for multi-area power systems: A new type-2 fuzzy approach based on Levenberg–Marquardt algorithm." *ISA transactions* 121 (2022): 40-52.

[5] Paliwal, Nikhil, Laxmi Srivastava, and Manjaree Pandit. "Application of grey wolf optimization algorithm for load frequency control in multi-source single area power system." *Evolutionary Intelligence* (2022): 1-22.

[6] Guha, Dipayan, Provas K. Roy, and Subrata Banerjee. "Equilibrium optimizer□tuned cascade fractional□order 3DOF□PID controller in load frequency control of power system having renewable energy resource integrated." *International Transactions on Electrical Energy Systems* 31, no. 1 (2021): e12702.

[7] Sahoo, Prafulla Kumar, Srikanta Mohapatra, Deepak Kumar Gupta, and Siddhartha Panda. "Multi verse optimized fractional order PDPI controller for load frequency control." *IETE Journal of Research* 68, no. 5 (2022): 3302-3315.

[8] Siti, M. W., D. H. Tungadio, N. T. Nsilulu, B. B. Banza, and L. Ngoma. "Application of load frequency control method to a multi-micro-grid with energy storage system." *Journal of Energy Storage* 52 (2022): 104629.

[9] Tripathi, Santosh, Vijay P. Singh, Nand Kishor, and A. S. Pandey. "Load frequency control of power system considering electric Vehicles' aggregator with communication delay." *International Journal of Electrical Power & Energy Systems* 145 (2023): 108697.

[10] Ahmed, Mohamed, Gaber Magdy, Mohamed Khamies, and Salah Kamel. "Modified TID controller for load frequency control of a two-area interconnected diverse-unit power system." *International Journal of Electrical Power & Energy Systems* 135 (2022): 107528.

[11] Guha, Dipayan, Provas Kumar Roy, and Subrata Banerjee. "Performance evolution of different controllers for frequency regulation of a hybrid energy power system employing chaotic crow search algorithm." *ISA transactions* 120 (2022): 128-146.

[12] Irudayaraj, Andrew Xavier Raj, Noor Izzri Abdul Wahab, Manoharan Premkumar, Mohd Amran Mohd Radzi, Nasri Bin Sulaiman, Veerapandiyan Veerasamy, Rizwan A. Farade, and Mohammad Zohrul Islam. "Renewable sources-based automatic load frequency control of interconnected systems using chaotic atom search optimization." *Applied Soft Computing* 119 (2022): 108574.

[13] Pathak, Pawan Kumar, Anil Kumar Yadav, Anshuman Shastri, and P. A. Alvi. "BWOA assisted PIDF-(1+ I) controller for intelligent load frequency management of standalone micro-grid." *ISA transactions* (2022).

[14] Shubham, Sourabh Prakash Roy, Ram Krishna Mehta, Arvind Kumar Singh, and Om Prakash Roy. "A novel application of jellyfish search optimisation tuned dual-stage (1+ PI) TID controller for micro-grid employing electric vehicle." *International Journal of Ambient Energy* 43, no. 1 (2022): 8408-8427.

[15] Mishra, Sonalika, Pratap Chandra Nayak, Umesh Chandra Prusty, and Ramesh Chandra Prusty. "Model predictive controller based load frequency control of isolated micro-grid system integrated to plugged-in electric vehicle." In *2021 1st Odisha International Conference on Electrical Power Engineering, Communication and Computing Technology (ODICON)*, pp. 1-5. IEEE, 2021.

[16] Guo, Jianping. "Application of a novel adaptive sliding mode control method to the load frequency control." *European Journal of Control* 57 (2021): 172-178.

[17] Wang, Zhenghao, and Yonghui Liu. "Adaptive Terminal Sliding Mode Based Load Frequency Control for Multi-Area Interconnected Power Systems With PV and Energy Storage." *IEEE Access* 9 (2021): 120185-120192.

[18] Bagheri, Amir, Ali Jabbari, and Saleh Mobayen. "An intelligent ABC-based terminal sliding mode controller for load-frequency control of islanded micro-grids." *Sustainable Cities and Society* 64 (2021): 102544.

[19] Safari, Amin, Farshad Babaei, and Meisam Farrokhifar. "A load frequency control using a PSO-based ANN for micro-grids in the presence of electric vehicles." *International Journal of Ambient Energy* 42, no. 6 (2021): 688-700.

[20] Mishra, Debashish, Pratap Chandra Nayak, Sushil Kumar Bhoi, and Ramesh Chandra Prusty. "Design and analysis of Multi-stage TDF/(1+ TI) controller for Load-frequency control of AC Multi-Islanded Micro-grid system using Modified Sine cosine algorithm." In *2021 1st Odisha International Conference on Electrical Power Engineering, Communication and Computing Technology (ODICON)*, pp. 1-6. IEEE, 2021.

[21] Latif, Abdul, SM Suhail Hussain, Dulal Chandra Das, and Taha Selim Ustun. "Double stage controller optimization for load frequency stabilization in hybrid wind-ocean wave energy based maritime micro-grid system." *Applied Energy* 282 (2021): 116171.

[22] Mohanty, Debidasi, and Sidhartha Panda. "Modified salp swarm algorithm-optimized fractional-order adaptive fuzzy PID controller for frequency regulation of hybrid power system with electric vehicle." *Journal of Control, Automation and Electrical Systems* 32, no. 2 (2021): 416-438.

[23] Fathy, Ahmed, and Abdullah G. Alharbi. "Recent Approach Based Movable Damped Wave Algorithm for Designing Fractional-Order PID Load Frequency Control Installed in Multi-Interconnected Plants With Renewable Energy." *IEEE Access* 9 (2021): 71072-71089.

[24] Roy, Sourabh Prakash, R. K. Mehta, A. K. Singh, and O. P. Roy. "A Novel Application of BESO-Based Isolated Micro-grid with Electric Vehicle." In *Sustainable Energy and Technological Advancements: Proceedings of ISSETA 2021*, pp. 597-609. Singapore: Springer Singapore, 2022.

[25] Sobhy, Mohamed A., Almoataz Y. Abdelaziz, Hany M. Hasanien, and Mohamed Ezzat. "Marine predators algorithm for load frequency control of modern interconnected power systems including renewable energy sources and energy storage units." *Ain Shams Engineering Journal* (2021).

[26] Sahu, Preeti Ranjan, Kumaraswamy Simhadri, Banaja Mohanty, Prakash Kumar Hota, Almoataz Y. Abdelaziz, Fahad Albalawi, Sherif SM Ghoneim, and Mahmoud Elsisi. "Effective Load Frequency Control of Power System with Two-Degree Freedom Tilt-Integral-Derivative Based on Whale Optimization Algorithm." *Sustainability* 15, no. 2 (2023): 1515.

[27] Arya, Yogendra. "Impact of hydrogen aqua electrolyzer-fuel cell units on automatic generation control of power systems with a new optimal fuzzy TIDF II controller." *Renewable energy* 139 (2019): 468-482.

[28] Alsattar, H. A., A. A. Zaidan, and B. B. Zaidan. "Novel meta-heuristic bald eagle search optimisation algorithm." *Artificial Intelligence Review* 53, no. 3 (2020): 2237-2264.

[29] Harifi, Sasan, Javad Mohammadzadeh, Madjid Khalilian, and Sadoullah Ebrahimnejad. "Giza Pyramids Construction: an ancient-inspired metaheuristic algorithm for optimization." *Evolutionary Intelligence* 14 (2021): 1743-1761.

[30] Das, Dulal Ch, A. K. Roy, and N. Sinha. "GA based frequency controller for solar thermal–diesel–wind hybrid energy generation/energy storage system." *International Journal of Electrical Power & Energy Systems* 43, no. 1 (2012): 262-279.

[31] Rao, R. Venkata, Vimal J. Savsani, and D. P. Vakharia. "Teaching–learning-based optimization: a novel method for constrained mechanical design optimization problems." *Computer-Aided Design* 43, no. 3 (2011): 303-315.

[32] Latif, Abdul, Dulal Chandra Das, Sudhanshu Ranjan, and Amar Kumar Barik. "Comparative performance evaluation of WCA-optimised non-integer controller employed with WPG–DSPG–PHEV based isolated two-area interconnected micro-grid system." *IET Renewable Power Generation* 13, no. 5 (2019): 725-736.

[33] Stine, William B., and Richard B. Diver. "A compendium of solar dish/Stirling technology." (1994).

[34] Kumari, Sandhya, and Gauri Shankar. "Maiden application of cascade tilt-integral–tilt-derivative controller for performance analysis of load frequency control of interconnected multi-source power system." *IET Generation, Transmission & Distribution* 13, no. 23 (2019): 5326-5338.

[35] Babaei, Masoud, Ahmadreza Abazari, and S. M. Muyeen. "Coordination between demand response programming and learning-based FOPID controller for alleviation of frequency excursion of hybrid micro-grid." *Energies* 13, no. 2 (2020): 442.

[36] Latif, Abdul, Dulal Chandra Das, Amar Kumar Barik, and Sudhanshu Ranjan. "Illustration of demand response supported co□ordinated system performance evaluation of YSGA optimized dual stage PIFOD□(1+ PI) controller employed with wind□tidal□biodiesel based independent two□area interconnected micro-grid system." *IET Renewable Power Generation* 14, no. 6 (2020): 1074-1086.

[37] Rasul, M. G., Chris Ault, and Mojibul Sajjad. "Bio-gas mixed fuel micro gas turbine co-generation for meeting power demand in Australian remote areas." *Energy Procedia* 75 (2015): 1065-1071.

[38] Muthu, D., C. Venkatasubramanian, K. Ramakrishnan, and Jaladanki Sasidhar. "Production of biogas from wastes blended with cowdung for electricity generation-a case study." In *IOP conference series: earth and environmental science*, vol. 80, no. 1, p. 012055. IOP Publishing, 2017.

[39] Pati, Subhranshu Sekhar, and Saroj Kumar Mishra. "A PSO based modified multistage controller for automatic generation control with integrating renewable sources and FACT device." *International Journal of Renewable Energy Research (IJRER)* 9, no. 2 (2019): 673-683.

[40] El-Fergany, Attia A., and Mohammed A. El-Hameed. "Efficient frequency controllers for autonomous two-area hybrid micro-grid system using social-spider optimiser." *IET Generation, Transmission & Distribution* 11, no. 3 (2017): 637-648.